Propagation Study in a Dense Urban Environment at the Sub-THz Band for Future Wireless Communications

Nektarios Moraitis, and Konstantina S. Nikita
Mobile Radiocommunications Laboratory, National Technical University of Athens and Institute of Communication and Computer Systems, Athens, Greece, morai@mobile.ntua.gr

***Abstract*—This paper presents the preliminary results of a propagation study at sub-THz frequencies considering line-of-sight (LOS) links in a dense urban environment. Path loss and wideband parameters are estimated and assessed through a deterministic simulation, using a software tool and a high-resolution digital map of the area. The study reveals that in street canyons reliable coverage can be provided up to 237 m at 140 GHz, provided that directional antennas are exploited in both terminals. In open spaces using omnidirectional and directional antennas at the terminals, wireless links can be established up to 140 m. The path loss can be predicted accurately by the close-in (CI) model, yielding path loss exponents 2.1 and 1.7, and standard deviations 2.2 and 1.8 dB, for open space and street canyons, respectively. Finally, the delay spread of the channel is found in the range of 2.7-24.0 ns, whereas the supported coherence bandwidth varies from 53 up to 178 MHz, thus indicating the frequency selective characteristics of the propagation channel.**

***Index Terms*—channel modeling, D-band, deterministic simulation, outdoor environment, path loss, sub-THz communications.**

I. Introduction

There is an ever-increasing demand for frequency spectrum to support high user densities, very low latencies and speeds that reach Tb/s in beyond fifth-generation (B5G) and the upcoming sixth-generation (6G) wireless networks [1], [2]. Currently, for the 5G networks there is a spectrum allocation in the sub-6 GHz band (FR1) and at the frequency bands of 26-28 GHz and 60 GHz (FR2). However, the available spectrum is limited and is expected to be congested in the years to come, being unable to fulfill the requirements of the next generation wireless networks.

To overcome these limitations the research community have envisaged to exploit sub-THz frequencies where a massive amount of spectrum is available and can easily support throughputs up to Tb/s [3]. However, the wireless links at those frequencies suffer from severe path loss and excess loss due to atmospheric absorption (oxygen and water vapor) [4]. Therefore, specific frequency regions should be allocated in order to minimize those losses. More specifically, the D-band region (110-170 GHz) has recently gained popularity, providing a vast bandwidth of 60 GHz [5].

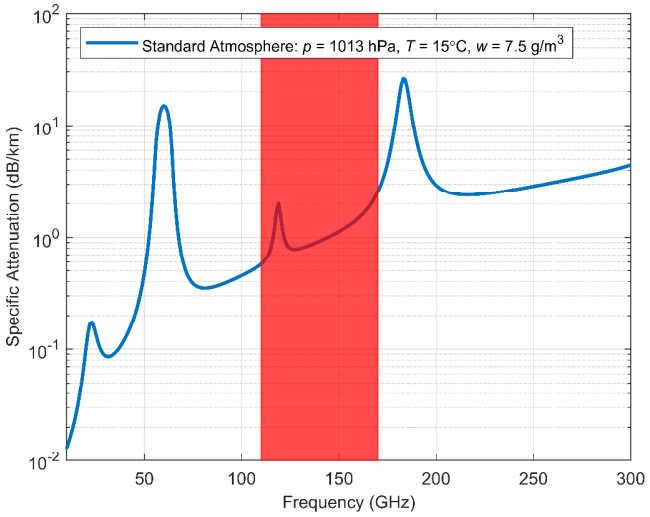

Fig. 1. Specific attenuation versus frequency spectrum for standard atmospheric conditions. The red rectangle indicates the D-band region.

The atmospheric absorption in the specific region is low where the specific attenuation remains below 2 dB/km, as one can observe in Fig. 1. The specific attenuation versus frequency in Fig. 1 was calculated according to [6].

In this context, it is a very intriguing task to assess the signal propagation above 100 GHz, especially in outdoor environments, where mainly directional short-range wireless links are expected to be used with the aim of compensating the increased path loss. Apart from path loss, it is also pivotal to study the wideband channel characteristics. There are limited research efforts that appear in the existing literature where measurement campaigns above 100 GHz are presented for outdoor environments [3]-[5] and [7]-[11]. The corresponding measurement campaigns are primarily focused on the characterization of the directional nature of the channel, presenting results for path loss and power angular spectrum. There are few papers that provide time delay parameters [8], [9].

The present work presents a propagation study based on simulations carried out at 140 GHz, considering a dense urban environment. The simulation is also performed as a complementary validation attempt, comparing the simulated results with existing measurements. The propagation

scenario involves line-of-sight (LOS) links where the transmitter (Tx) and receiver (Rx) are placed below rooftop. Open space area and street canyon propagation are assessed for different antenna combinations, delivering, apart from the path loss results, the time delay parameters of the channel.

The rest of the paper is structured as follows. The simulation environment and procedure are outlined in Section II. The processing of the simulated data and the extraction of the wideband parameters are described in Section III. The path loss analysis and the time delay results of the simulated channel are delivered and discussed in Section IV, followed by a brief conclusion in Section V.

II. Simulation Environment and Procedure

The propagation study was carried out using a software tool (Advanced Topographic Development & Images, "ICS Telecom" [12]), which, with the help of 3D digital maps, delivers numerous propagation analyses up to 300 GHz. The high-resolution digital terrain map (DEM) was acquired from aerial photographs. The simulation takes into consideration a dense urban environment, downtown Athens, Greece. The digital map has a resolution better than 1 m and represents all buildings' outlines and heights. The simulated environment is about 10 km^2, part of Athens city center, with six or seven storey buildings. There are narrow streets (about 8-10 m wide) that form propagation canyons, and also central avenues (about 32 m wide). The average building height was in the range of 18-25 m.

Fig. 2 depicts two parts of downtown Athens where two different scenarios were examined. Both scenarios represent a LOS below-rooftop propagation condition. The first (Scenario 1), shown in Fig. 2(a), is an open space area (square) where the Tx is placed in the middle and various Rx positions are selected around. The second scenario (Scenario 2), presented in Fig. 2(b), involves a street canyon, where the Tx is located in the middle of the street with different Rx positions selected along. The distance between Tx and Rx in both scenarios varies from 41 to 237 m. The Tx height is assumed to be 10 m above the ground (e.g., mounted on lampposts), whereas the Rx height is selected 1.7 m above the ground in every location and scenario. It is worth remarking that the trees appearing in the maps are not included in the digital map during the simulation procedure.

The analysis was conducted at 140 GHz. In Scenario 1, a biconical antenna with a gain of 2 dBi was selected at the Tx, which was omnidirectional in azimuth plane with a 3-dB beamwidth of 60◦ in the elevation plane [4]. A directional horn antenna was assumed in the Rx, with a gain of 19 dBi and a 3-dB beamwidth of 40◦ in azimuth and elevation planes, respectively. The Rx antennas were always pointing at the Tx so as to maximize the gain and compensate the excess losses. In Scenario 2, directional antennas of 21 dBi gain were assumed for both Tx and Rx terminals, with a 3-dB beamwidth of 20◦ in azimuth and elevation planes, respectively.

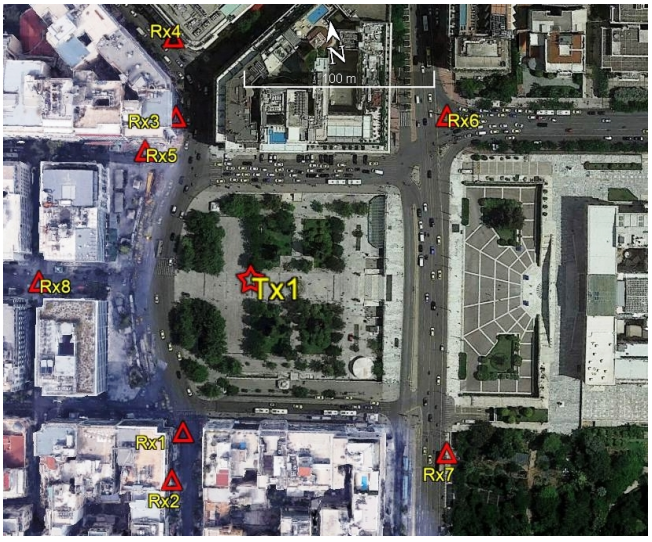

(a)

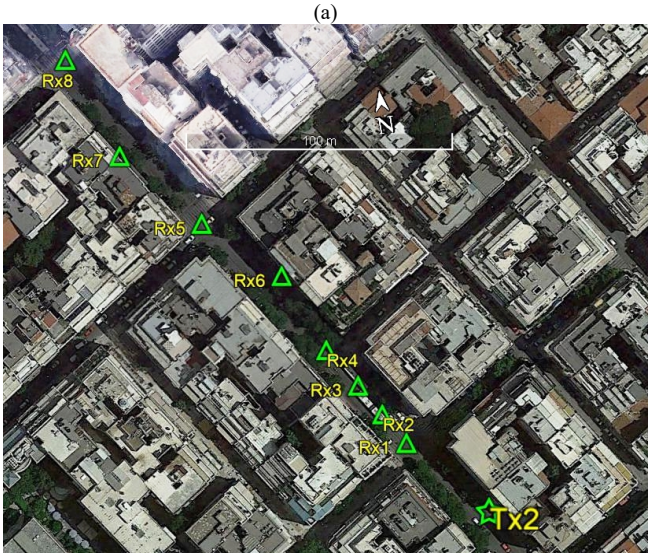

(b)

Fig. 2. Propagation study environment in parts of downtown Athens. (a) Scenario 1. (b) Scenario 2. The photos are taken from Google Earth™. The trees appearing in the area are not embedded in the digital map during the simulation procedure.

The Tx and Rx antennas were also pointing at each other. All the antennas were assumed to have vertical polarization, whereas a Tx output power of 10 dBm was considered. A transmitted bandwidth of 2 GHz was also considered that corresponds to a time resolution of 0.5 ns.

The software tool produces a fully deterministic simulation where the buildings appear as physical obstacles to the signal propagation. Wideband scenarios can be also simulated utilizing the 3D ray-tracing module of the software, thus resolving the destructive and constructive field strength effects that depend on the time of arrival difference between the direct and the reflected components. The power delay profile and delay spread can be also estimated [13], [14]. Based on the ray tracing technique, the tool determines all the direct and reflected paths in the propagation area and

generates an output file with power-delay samples. Finally, the power received at each Rx location is calculated.

III. Data Processing

As mentioned in Section II, the simulation tool produces the power-delay samples, or the power delay profile (PDP) of the channel that is expressed as

$$P(\tau) = \left|h_b(\tau)\right|^2 = \sum_k a_k^2(\tau)\delta(\tau - \tau_k) \qquad (1)$$

where a_k^2 and τ_k are the power-delay samples, respectively, of the k-th multipath component and $\delta(\cdot)$ stands for the unit impulse function, and $h_b(\tau)$ denotes the baseband impulse response of the channel. Data reduction is applied to the generated PDP samples to extract the power-delay samples that produce appropriate results. A data binning procedure is performed where each PDP is quantized into bins of 0.5 ns and within each bin the power values are averaged producing an equivalent power A_K^2 at T_K time delay [15]. The final reduced PDP is given by

$$P(\tau) = \sum_K A_K^2(\tau)\delta(\tau - T_K) \qquad (2)$$

Then, each PDP is normalized to its power gain $P_{\text{norm}}(\tau) = P(\tau)/G_r$, where $G_r = \sum_K A_K^2(\tau)$ and a threshold of -30 dB below the maximum is imposed [16]. From equation (2), the maximum delay (MD), the mean excess delay (MED) and the rms delay spread (DS) of the channel are calculated. Details for those parameters and their corresponding expressions can be found in [17], [18].

The received power at each Rx location is then used to calculate the path loss. De-embedding the antenna gains, the path loss, in decibels, is expressed as

$$PL(d) = P_{Tx} + G_{Tx} + G_{Rx} - P_r(d) \qquad (3)$$

where d is the distance between Tx and Rx in meters, G_{Tx} and G_{Rx} denote the Tx and Rx antenna gains in dBi, respectively, P_{Tx} stands for the Tx output power in dBm, and finally, P_r denotes the received signal power, in dBm, at each Rx location at distance d from the Tx.

IV. Results and Discussion

First, path loss results are assessed and modeled for each examined scenario. Path loss provides valuable information about the coverage range of the wireless link. Fig. 3 illustrates the simulated path loss versus distance, where at the maximum distance of 237 m in Scenario 2 a path loss of 113 dB (-66.7 dBm received power) was estimated.

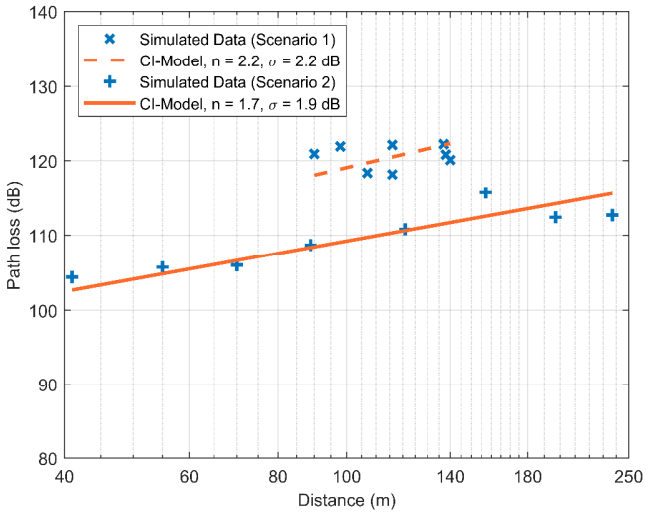

Fig. 3. Path loss versus distance for both examined scenarios. The CI-model is fitted to the simulated path loss data.

The maximum path loss is about 122 dB and is observed in Scenario 1 at a distance of 137 m. The path loss value at the maximum distance of 140 m is equal to 120 dB. Therefore, omnidirectional picocells can also operate in open spaces without any problem, yet directional antennas should be adopted in the Rx in order to avoid the excess losses.

A widely adopted model that is used to characterize path loss is the close-in (CI) path loss model with 1 m reference distance [8]. The modeled path loss, in decibels, is expressed as

$$PL^{\text{CI}}(d) = PL_{FS} + 10n\log_{10}\left(\frac{d}{d_0}\right) + x_\sigma \qquad (4)$$

where d is the distance in meters between Tx and Rx, n is the path loss exponent, d_0 is the reference distance (selected 1 m) and PL_{FS} is the free space path loss, in decibels, given by

$$PL_{FS} = 20\log_{10}\left(\frac{4\pi d_0}{\lambda}\right) \qquad (5)$$

with λ being the wavelength in meters. Finally, x_σ in (4) is the shadow fading that is modeled by a zero mean Gaussian variable with standard deviation σ in decibels. The specific model is fitted to the simulation data as shown in Fig. 3, where low errors are obtained. The path loss exponent value in Scenario 1 is found equal to 2.1 with σ = 2.2 dB. The corresponding values for Scenario 2 are n = 1.7 and σ = 1.8 dB. The exponent in Scenario 1 (open space area) is slightly higher than that of free space (n = 2) due to the presence of the omnidirectional antenna at the Tx which generates multiple reflected components that arrive at the Rx. These probably increase the rate of destructive interference, thus deteriorating path loss. In Scenario 2 the corresponding exponent, which is lower than 2, implies a typical waveguide

effect due to the canyon propagation, formed by the tall buildings that surround the Rx.

Based on the obtained results, it is evident that the CI model can accurately predict path loss for wireless links at 140 GHz. The results are of the same order of magnitude with those reported in [4], [7], and [8], where the path loss exponent and σ for LOS omnidirectional links are found equal to 1.9 and 2.7 dB, respectively. For directional links these parameters are found equal to 2.1 and 2.8 dB, respectively.

Furthermore, it is important to assess the wideband channel characteristics and its time delay parameters. Fig. 4 presents, the produced PDPs for two indicative Rx locations for both scenarios. In Scenario 1 (Omni/Directional antennas) the PDP is found wider than that of Scenario 2 (Directional/Directional antennas), as one can observe in Fig. 4. In Scenario 1, the MD, MED and DS values are equal to 187, 7.3, and 23.7 ns, respectively, whereas in Scenario 2, the corresponding values are found 24.5, 1.5, and 2.7 ns. It is obvious that in Scenario 2 the DS is reduced as compared with Scenario 1. This implies that in street canyons the LOS component dominates the signal propagation with few other multipath components to exist (e.g., reflections from the ground and building facades), when narrow-beam antennas are used for LOS links in sub-THz bands. On the other hand, in open space areas (Scenario 1) apart from the LOS component, there exist many multipath components due to the omnidirectional antenna at the Tx and the wide-beam antenna at the Rx, thus increasing the excess delay.

The time delay parameters are comparable with those reported in [7] where in simulated LOS omnidirectional links the MD is found equal to 132 ns, with a DS of 37.6 ns. Furthermore, for narrow-beam LOS directional links, the DS ranges between 0.7 and 13.9 ns [8], [9]. Table I summarizes the produced wideband parameters of the channel, for each scenario and Rx location. The DS ranges from 14 to 24 ns, for Scenario 1 and from 2.7 to 10.6 ns for Scenario2, being consistent with the values found in the existing literature. Furthermore, the DS values increase in cross sections, in Scenario 2 (e.g., Rx1 and Rx5), as well as in the wider streets of Scenario 1 (e.g., Rx5-Rx8) compared with the rest of the locations. This infers that the receiver collects reflections from the building facades with longer delays (the rays travel longer distances in wider openings), increasing thus the DS values.

As it is evident in Table I, the DS values are slightly lower than MED for the majority of the selected locations, and the spreading factor (i.e., the ratio between MED and DS) is equal to 1.1, on average. In both scenarios, the produced PDPs contain many weak reflections in the late time (that greatly affect DS), whereas they are dominated by strong multipath components in early time (that influence MED).

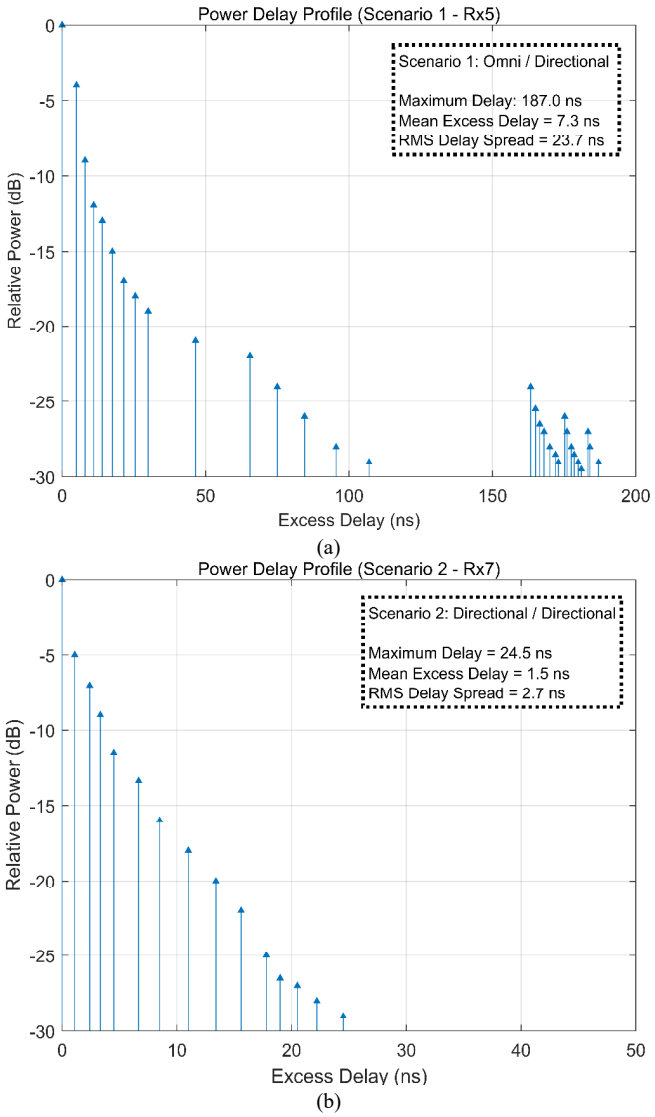

Fig. 4. Indicative power delay profiles from two Rx locations. (a) Scenario 1. (b) Scenario 2.

Applying a Fourier transform to each PDP one can yield the frequency correlation function (FCF) of the propagation channel. This provides valuable knowledge for the frequency selectivity of the channel accounting for the coherence bandwidth capability [18]. Selecting a correlation level of 50%, the coherence bandwidth (C_{BW}) is calculated in MHz, and the results are also summarized in Table I. The coherence bandwidth is found in the range of 53-69 MHz in Scenario 1, being more than double in Scenario 2, taking values between 105 and 178 MHz. In any case, the yielded values indicate that the channel at 140 GHz exhibits frequency selective characteristics and justify the calculated values of the DS. In Scenario 1, the higher delay parameters result in low coherence bandwidth, whereas the opposite stands for Scenario 2, where the channel demonstrates higher frequency coherence.

TABLE I. WIDEBAND PARAMETERS OF THE 140-GHZ CHANNEL.

Scenario	Rx #	d_{Tx-Rx} [m]	MD [ns]	MED [ns]	DS [ns]	C_{BW} [MHz]
1 Omnidirectional / Directional	1	90	95	18	16	69
	2	116	91	17	16	69
	3	98	101	19	17	65
	4	138	98	16	14	79
	5	107	187	7.3	24	53
	6	137	125	21	19	58
	7	140	123	21	18	62
	8	116	131	24	21	53
2 Directional / Directional	1	41	39	11.3	10.1	110
	2	55	28	7.9	7.0	159
	3	70	30	8.9	7.5	148
	4	89	28	8.2	7.6	146
	5	157	41	11.5	10.6	105
	6	121	33	9.5	8.6	129
	7	197	25	1.5	2.7	178
	8	237	29	8.4	7.9	141

Finally, at 140 GHz, rain is expected to attenuate further the wireless link. The specific attenuation due to rain in (dB/km) is calculated according to [19], considering a rain rate of 47.5 mm/h, for 0.01% of time in the Athens region. Assuming vertical polarization, the specific attenuation is found 19.1 dB/km. The maximum achieved distance in Scenario 2 is 237 m, which entails an excess attenuation of 12.8 dB due to rain. This excess loss is not prohibitive for establishing viable links at 140 GHz, provided that highly directional antennas are used and short-range cells are adopted.

V. CONCLUSION

The current work presented preliminary results of the path loss and wideband channel characteristics based on simulations in a dense urban environment at 140 GHz. Two different scenarios were examined with different antenna combinations for LOS and below-rooftop wireless links. The results revealed that viable coverage can be established in open space and street canyons up to 237 m. Furthermore, successful predictions of the path loss were produced by the CI model leading to path loss exponents of 2.1 and 1.7, and low standard deviations of 2.2 and 1.8 dB, in open space and street canyons, respectively. The delay parameters of the channel validated its frequency selective characteristics where the delay spread was found in the range of 2.7-24.0 ns. Finally, coherence bandwidths up to 178 MHz can be supported in street canyons employing directional antennas at both terminals.

As future work, the authors intend to carry out further simulations considering non-LOS links in outdoor locations, examining different location scenarios and antenna selections. The ultimate goal is to provide a versatile model of the PDP, the delay clusters, and the inter-arrival time of the multipath components for the wireless channel at 140 GHz.

REFERENCES

[1] H. Viswanathan and P. E. Mogensen, "Communications in the 6G Era," *IEEE Access.*, vol. 8, pp. 57063-57074, Mar. 2020.

[2] I. F. Akyildiz, A. Kak, and S. Nie, "6G and beyond: The future of wireless communications systems," *IEEE Access*, vol. 8, pp. 133995-134030, Jul. 2020.

[3] N. A. Abbasi *et al.*, "Double directional channel measurements for THz communications in an urban environment," in *Proc. IEEE Int. Conf. Commun. (ICC)*, Dublin, Ireland, Jun. 2020, pp. 1-6.

[4] Y. Xing and T. S. Rappaport, "Propagation measurement system approach at 140 GHz - Moving to 6G and above 100 GHz," in *Proc. IEEE Global Commun. Conf. (GLOBECOM)*, Abu Dhabi, United Arab Emirates, Dec. 2018, pp. 1-6.

[5] T. S. Rappaport *et al.*, "Wireless communications and applications above 100 GHz: Opportunities and challenges for 6G and beyond," *IEEE Access*, vol. 7, pp. 78729-78757, Jun. 2019.

[6] International Telecommunication Union, "Attenuation by atmospheric gases and related effects," Geneva, Switzerland, Rec. ITU-R P.676-13, Aug. 2022.

[7] Y. Xing and T. S. Rappaport, "Propagation measurements and path loss models for sub-THz in urban microcells," in *Proc. IEEE Int. Conf. Commun. (ICC)*, Montreal, QC, Canada, Jun. 2021, pp. 1-6.

[8] Y. Xing and T. S. Rappaport, "Millimeter wave and terahertz urban microcell propagation measurements and models," *IEEE Commun. Lett.*, vol. 25, no. 12, pp. 3755-3759, Dec. 2021.

[9] S. Ju and T. S. Rappaport, "140 GHz urban microcell propagation measurements for spatial consistency modeling," in *Proc. IEEE Int. Conf. Commun. (ICC)*, Montreal, QC, Canada, Jun. 2021, pp. 1-6.

[10] B. De Beelde, E. Tanghe, D. Plets, and W. Joseph, "Outdoor channel modeling at D-band frequencies for future wireless access appplications," *IEEE Wireless Commun. Lett.*, Early Access, Aug. 2022.

[11] Y. Xing and T. S. Rappaport, "Terahertz wireless communications: co-sharing for terrestrial and satellite systems above 100 GHz," *IEEE Commun. Lett.*, vol. 25, no. 10, pp. 3156-3160, Oct. 2021.

[12] Advanced Topographic Development & Images, "ICS Telecom - Comprehensive Network Engineering on V/U/SHF Bands," [Online]. Available: http://www.atdi.com.

[13] Grenier, "Signal propagation modeling in uran environment," ATDI White Paper, June 2005.

[14] T. Garand, "Multipath in ICS telecom," ATDI White Paper, Jan. 2005.

[15] N. Moraitis and P. Constantinou, "Measurements and characterization of wideband indoor radio channel at 60 GHz," *IEEE Trans. Wireless Commun.*, vol. 5, no. 4, pp. 880-889, Apr. 2006.

[16] N. Moraitis, A. Panagopoulos, and I. Popescu, "Propagation study of a wideband SIMO land mobile satellite system in a dense urban environment," in *Proc. 8th European Conf. Antennas Propag. (EuCAP)*, The Hague, The Netherlands, Apr. 2014, pp. 1680-1684.

[17] T. S. Rappaport, *Wireless Communications: Principles and Practice*, 2nd ed. Upper Saddle River, NJ: Prentice Hall, 2002.

[18] A. F. Molisch, *Wireless Communications*, 2nd ed. West Sussex, UK: John Wiley & Sons Ltd., 2011.

[19] International Telecommunication Union, "Specific attenuation model for rain for use in prediction methods," Geneva, Switzerland, Rec. ITU-R P.838-3, Mar. 2005.